九州大学学術情報リポジトリ
Kyushu University Institutional Repository

Preparation And Characterization of MCM-41 Membrane for Biogas Purification

Saputra, Hens
Research Center for Process and Manufacturing Industry Technology, National Research and Innovation Agency

Husodo, Dwi
Research Center for Process and Manufacturing Industry Technology, National Research and Innovation Agency

SD. Sumbogo Murti
Research Center for Process and Manufacturing Industry Technology, National Research and Innovation Agency

Semuel Pati Senda
Research Center for Process and Manufacturing Industry Technology, National Research and Innovation Agency

https://doi.org/10.5109/7151735

出版情報：Evergreen. 10 (3), pp.1855-1861, 2023-09. Interdisciplinary Graduate School of Engineering Sciences, Kyushu University, Japan
バージョン：
権利関係：Creative Commons Attribution-NonCommercial 4.0 International

KYUSHU UNIVERSITY

Preparation And Characterization of MCM-41 Membrane for Biogas Purification

Hens Saputra[1,*], Dwi Husodo[1], SD. Sumbogo Murti[1], Semuel Pati Senda[1]
[1]Research Center for Process and Manufacturing Industry Technology,
National Research and Innovation Agency, Jakarta 10340, Indonesia

E-mail: hens.saputra@brin.go.id

(Received April 28, 2023; Revised July 7, 2023; accepted July 20, 2023).

Abstract: The inorganic membrane MCM-41 (Mobile Compound Material) is introduced as a purification method for biogas. In this experiment, the tertiary ammonium surfactant, cethyltrimethylammonium bromide (CTAB) as an organic template, tetraethylortosilicate (TEOS) as a source of silica, hydrochloric acid (HCl) as a catalyst, deionized water (H_2O), and ethanol (C_2H_5OH) were used to create the MCM-41 membrane. X-ray diffraction (XRD), scanning electron microscopy (SEM), gas permeability, physisorption, pore size distribution, and BET (Brunauer-Emmett-Teller) surface area were used to describe the produced membrane. This membrane has excellent thermal stability, a small pore size distribution, pores that are on average around 2 nm in size, a large specific surface area of 1200 m^2/g, and pores that are 1.08 cm^3/g in volume. The gas separation mechanism in membrane showed the Knudsen flow, indicating the existence of mesoporous structure. This membrane is recommended for biogas plant in separation of CH_4 and CO_2.

Keywords: membrane; MCM-41; biogas; upgrading, methane

1. Introduction

Currently, The fuel that used in daily life is primarily supplied by fossil fuels. The fossil fuel resources are getting limited. In the other hand, the carbon dioxide emissions from fossil fuels causes environmental damage and global warning[1,2]. Energy challenges and issues that various nations, including Indonesia, are currently dealing with dependence on imported fuels, inefficient energy consumption, and poor utilization of novel and renewable energy sources[1]. The burning of fossil fuels for industry and electricity generation is linked to an increase in CO_2 levels in the atmosphere. In the Paris Agreement against Climate Change, countries agreed to reduce their CO_2 emissions.[3]. Indonesia has set target of emission reduction and net zero emission by 2060.[4] Some research about green technology to reduce emission and achieve green energy has been conducted. One of the renewable energy sources, biogas, has the potential to take the place of natural gas as a fuel and a raw material in a number of industries. Biogas could be produced via anaerobic digestion of organic wastes. Biogas often contains CO_2, H_2, H_2S, and N_2 in trace proportions, as well as trace amounts of CH_4 (50–70% vol), CO_2 (30-38%vol) and other gases.[5] The radiation-absorbing properties of high CO_2 reduce cylinder temperature and postpone expansion to a crank angle of 10–20° after top dead center[6]. The potential biogas from palm oil milled effluent (POME) in Indonesia was about 490 million cubic meter per year[3].[7] The purified biogas could be used directly as fuels for car or truck and in gas engine to produce electricity[8,9]. There are many techniques to improve the quality of biogas. The potential use of membranes, particularly in gas separation applications such as gas separation for CO_2 removal in natural gas, upgrading biogas, producing dry air, etc[5,10,11]. In water scrubber, increasing the contact area between biogas and water was needed to improve the effectivity by filling the scrubber with random packing. On the one hand, the addition of packing can block the scrubber, which means the pressure will increase. This causes the energy used to go up, and it can also cost to upgrade the biogas system[12].

Membrane technology covers a very wide application, such as separation and purification for liquid or gas, electronic devices i.e. sensor, battery, etc. The potential application of membranes especially in gas separation such as gas separation for CO_2 removal in natural gas, biogas upgrading, oxygen generator, nitrogen concentrator, dry air production, etc.[13,14,15] There are two types of membranes: organic membranes made from polymers, and inorganic membranes made from materials like metals. Polymers can be used to create membranes, but only a few of them work well in practice because of their chemical and physical properties. The polymeric membranes have merits such as low risk in production (e.g. cheap and simple) but they don't have endurance against

high temperature, mechanical strength and chemicals. Membranes can be damaged by things like non-aqueous organic solvents, dry atmospheres, or high temperatures. This can cause the membrane to collapse and lose its ability to filter things. Some things like high or low pH might also cause the membrane to break down and be destroyed by enzymes from bacteria. There are some disadvantages to using organic membranes, but inorganic ones are more stable and can be used in a wider variety of applications.[16].

There are several inorganic membranes materials such as metals, glasses, and ceramics. These materials are very stable and can be used in high-temperature membrane processes or in areas with high pH levels. This means that it can be used either directly or together with microbes. Characteristic of inorganic membranes could support the upgrading process of biogas[17].

In natural ecosystem, biogas was produced at low pH i.e. 3-5.[18] The acetate converts into CH_4 and CO_2 in reactor as function of pH. The previous research high pH could increase the CH_4 content up to 79%. The utilization of inorganic membrane could reduce the cost and carbon footprint than the conventional one.[19]

Mesoporous materials that are known as M41S have a lot of small, uniform channels with large surface areas. It can be controlled how wide the channels are by using different surfactants, chemicals, and reaction conditions. The M41S family of materials have different types of pores that are arranged in different ways. Materials can have three different types of pores: one-dimensional hexagonal pores, such as those found in MCM-41, three-dimensional cubic pores, such as those found in MCM-48, and an unstable lamellar structure, such as those found in MCM-50. The synthesis of the M41S family involves the use of a structure-directing surfactant, a solvent, a source of silica, and a acid or base catalyst. This paper is focused on the study of synthesis and characterization of MCM-41 inorganic membrane, transport mechanism of gas and prospect its application for upgrading biogas.[20] This paper was focused on preparation and characterization of MCM-41 membrane for biogas upgrading to produce bio methane/bio CNG (Compressed Natural Gas).

2. Experimental

On an asymmetrically structured flat porous alpha alumina disk, which served as the support, the MCM-41 inorganic membrane was created. The upper layer's pores have an average diameter of about 100 nm. The alumina support was treated with ethanol and deionized water, then dried. The parent solution was created using tetraethyl orthosilicate (TEOS), quaternary ammonium surfactant, $C_{16}H_{33}(CH_3)_3$ NBr, hydrochloric acid, ethanol, and deionized water. The mother solution of MCM-41 membrane was prepared using molar ratio as follows : 1,0 TEOS: 0,05 CTAB: 0,5 HCl: 25 C_2H_5OH and 75 H_2O. For 30 minutes, the mixture was agitated at 200 rpm at 30 °C. The alumina support then dip into parent solutions then water content was removed at 100 °C for 1 hour. After that, it was calcined for an hour at 600 °C with a 1 °C per minute heating rate. Figure 1 depicts the preparation procedure for the inorganic membrane MCM-41 in a flow diagram.

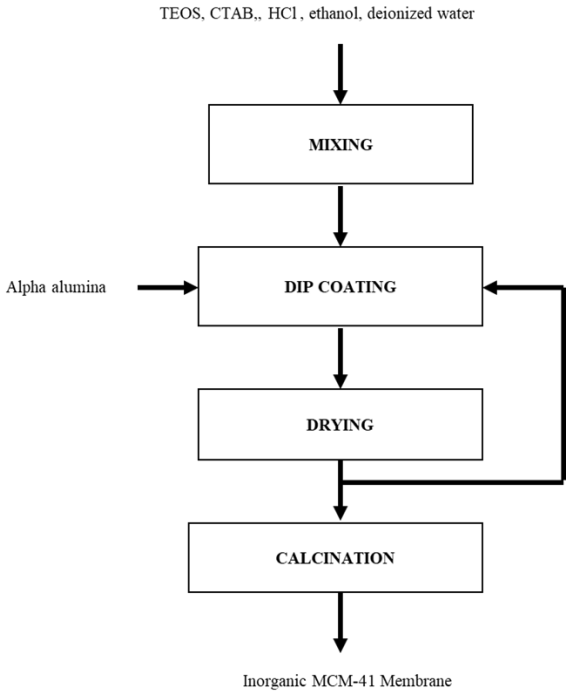

Fig. 1: The Diagram of MCM-41 membrane preparation

The structure of synthesized membrane was analyzed by X-ray diffraction (XRD) using Cu Kα radiation λ=1.540 Å (Philips X's Pert-MRD). Further more microstructure of membrane was characterized using a JEOL Co., Ltd. scanning electron microscope (SEM), model JED-2100. Characteristic of pores and gas transport mechanism in membrane was analyzed using nitrogen adsorption-desorption isothermal at 44 K, Quantachrome AUTOSORB-1 and gas permeation. Pores on a membrane are very sensitive to the size and shape of the pores, as well as the connectivity of the pores. This sensitivity determines how much fluid (or gas) can be moved through the membrane per unit difference in pressure. The permeability (or permeance) of a membrane is a measure of this ability. Permeability is usually expressed in terms of kilograms of fluid (or gas) moved per liter of pressure difference, called permselectivity. The permeability of two gases is usually called permselectivity to the membrane. The permeability, P, of a weakly adsorbed gas, such as helium, through a membrane can be used to calculate the gas diffusion coefficient. The measurements of gas permeation were conducted at 300-873 K of temperature range, and 123 kPa of pressure. The rate of each gas's escape from the interior of the membrane tube at atmospheric pressure was gauged using a sensitive bubble flow meter.

The permeation experiment was conducted at room

temperature. For more accurate readings of permeability, the gas was also measured with a GC-TCD (gas chromatograph with thermal conductivity detector). The flow rate of gas coming out of the tube on the side of the container was measured with a bubble flow meter. The gas was then injected into a gas chromatography machine to determine the concentration of the gas that was permeated. The steady state flux of the pure component can be evaluated from the pressure and time response of transducer. The active area of membrane for permeation was 1 cm^2. The flux of permeate gas was observed and utilized to calculate the permeance.

Physisorption isothermal was conducted by using Quanta chrome Autosorb-1. This equipment is capable of measuring nitrogen adsorption or desorption at relative pressures (*p/po*) between 0.001 and 1.0. The adsorption and desorption isotherm of inert gas, like N_2, at 77 K is determined by what pressure it is under. The isotherm is a curve that shows how the adsorption and desorption rates change with pressure. This is to find out the gas concentration (p/p^0) in the sample that can be measured using a volumetric gravimetric method. The information was gathered from a cell that contained a solid adsorbent and was maintained at a temperature that was below the adsorbent's critical temperature. The pressure inside the cell fluctuated as adsorption or desorption took place until it achieved equilibrium. The amount of gas that was added to or taken away from the vicinity of the adsorbent was utilized to calculate the quantity of gas required to fill the vicinity of the adsorbent. Because the vapor pressure could be monitored for each data point, P/P0 could be calculated with a high degree of accuracy and precision that was gathered for the measurement of the saturation pressure during the investigation. The adsorbed quantity are presented as volume (STP). Before each sorption calculation, the sample was outgassed at 573 K for 1 h under a turbo molecular pump vacuum.[21)]

A solid object's surface area can be measured using the Brunauer-Emmett-Teller (BET) method. In order to use this method, a linear plot of $1/[W(p^0/p)-1]$ versus p/p^0 in the vicinity of p/p^0 0.04 to 0.35 is needed. However, for microporous materials, the pressure in the linear region is lowered to make sure accurate results can be obtained. Total of surface area of the sample was obtained from the calculation of mol times Avogadro's number and cross-sectional area of nitrogen i.e. 16.2 $Å^2$ then divide by the molecular weight of the adsorbed.

Assuming that the pores are filled with a liquid that has been adsorbed and that the solid has no macropores, the total pore volume is determined. If the material does really have macropores, the isotherm will rise swiftly close to 1 p/p^0, and with careful temperature control, the total pore volume can be estimated with accuracy. The limiting adsorption at the boundary of bulky macropores, however, may be reliably determined with the total pore volume assuming certain temperature control of the sample. This is because the isotherm increases quickly around $p/p^0=1$ when bulky macropores are present.

There is general agreement that the desorption isotherm is a better way to find out pore size distribution than using the adsorption isothermal method. The desorption branch of the isotherm exposes a lower pressure, which concludes in a bring-down liberated energy state. This means the desorption isotherm is nearer to actual thermodynamic stability. The adsorption of adsorbates and adsorbents is classified according to the strength of the forces involved. Low enthalpy defines physical adsorption, which includes weaker forces including van der Waals forces, London forces, and polar contacts. Chemical adsorption, which outcome in the arrangement of a monolayer of adsorbate on the adsorben, occurs when adsorbates and adsorbents interact through chemical bonding. A thin adsorbate coating is created on the adsorbent as a result of physisorption. The more adsorbate there is, the more layers of it will be formed[22)].

To ensure the active pore of membrane, permporometry analysis was carried out. While the passive holes are inactive and make no contribution, the active pores enable effective gas diffusion. The only technique that is currently suitable for determining the size distribution of the active pores in porous media with diameters ranging from around 1.5 to 100nm is permporometry. This is specially important for porous media with an asymmetric structure. This technique measures the gas flux through the membrane's remaining open holes by using the controlled occlusion of pores caused by capillary condensation of vapor, which is a component of the gas mixture. Pore size is determined by the long-familiar phenomenon of capillary condensation of a liquid inside a porous medium. The pressure of condensed liquid in a small pore in a liquid-gas interface is related to the curvature of the interface and can be accurately represented by Kelvin's relation. Starting from the minimum in diffusional transport when relative pressure equal to 1, then the relative pressure was decreased to zero, at the same time the diffusional flux of nitrogen through membrane is measured with gas chromatograph. In this way a desorption isotherm is acquired, given in term of nitrogen flux at various relative pressure of water.

3. Results and Discussion

The synthesized membranes had been analyzed by XRD using Cu Kα radiation. Based on Figure 2. that the membrane shows XRD pattern of the MCM-41 structure for 3 times dip coating and after calcination at 600 °C for 1 hour was clearly observed by the highest peak of (100) and three others small peaks (110), (200) and (210). The MCM-41 structure exhibits the visual aspect of an overwhelming diffraction peak at 2.4° with the plant (100) indicated ordered porous structure. Other weak diffraction peak at 3,6°, 4.3° and 5.4°. Which corresponds to the planes (110), (200) and (210) was verify the mesoporous structure. The MCM-41 structure was still observed clearly after calcination at 600 °C, indicating a good

stability structure at high temperature[23].

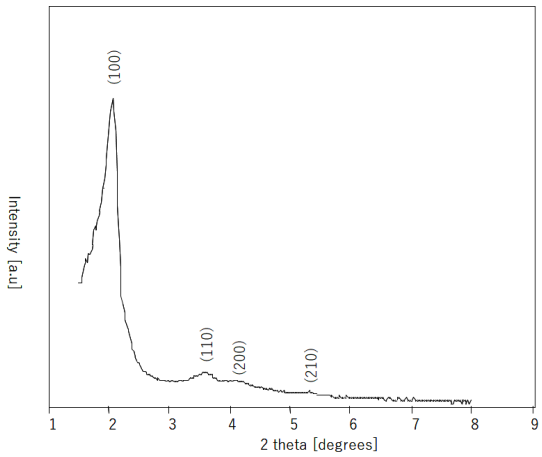

Fig. 2: XRD pattern of synthesized MCM-41 membrane (3 times dip coating)

Nitrogen adsorption-desorption isothermal experiment at 44 K results was showed at Figure 3. There was no hysteresis at the graph of nitrogen adsorption and desorption isothermal. This phenomenon was indicating

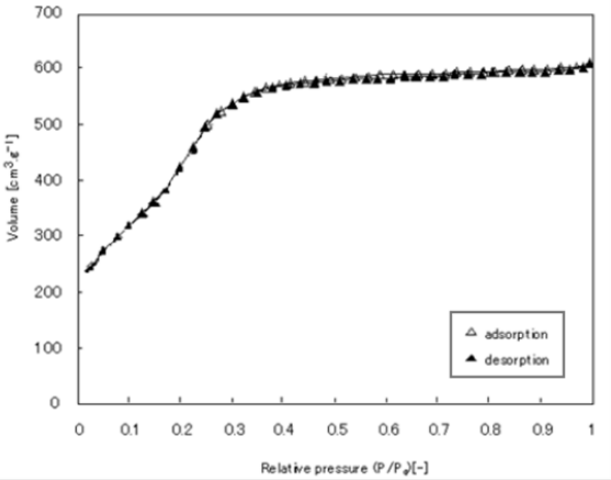

Fig. 3: Adsorption-desorption isothermal nitrogen in MCM-41 membrane

the same pore size at outside and inside of pores. The physical phenomenon loop related to capillary condensation.

Adsorption hysteresis is crucial for both the network effect of pore structure and adsorption stability. This is especially true for nanoporous medium, where pore blockage can have an impact on the desorption branch of the isotherm [21].

The relative vapor pressure (*p/po*) ranged from 0 to 1. The increase in the nitrogen adsorption curve from 0.2 to 0.5 relative vapor pressure indicates the membrane has a mesoporous structure. This data was supported by curve of desorption showed the significant decrease at the same area of increasing curve of adsorption. The sharp increase as seen at 0.2 to 0.5 is due to capillary nitrogen condensation in the mesoporous. The sharp inflection indicates homogeneous pore size and height, which points to a high pore volume [24].

Barrett Joyner Halenda (BJH) pore size distribution could be calculated as shown at Figure 4. With an average BJH pore size of only 2 nm, the membrane exhibits a restricted pore size dispersion. BET had pore volumes of 1.08 cm3/g and 1200 m^2/g, respectively. High porosity and pore volume of the membrane was also observed clearly form Scanning Electron Microscope (SEM) image as shown in Figure 5. The MCM-41 membrane had a thickness of around 20 m.

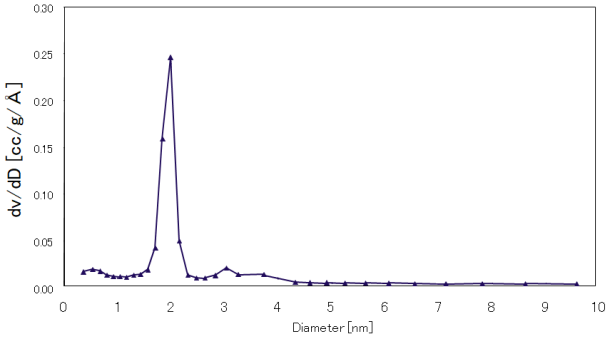

Fig. 4: Distribution of BJH pores in the MCM-41 membrane

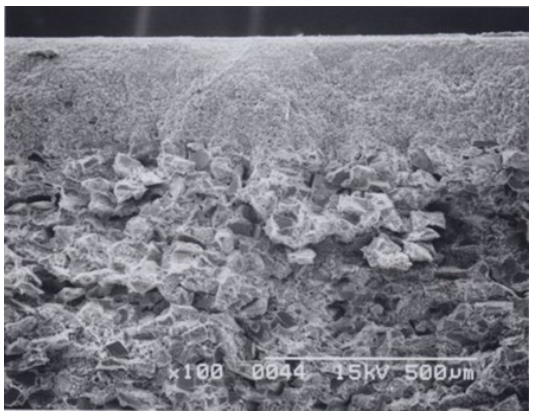

Fig. 5: SEM image of membrane

Transparent at room temperature, gas permeation testing shows that before calcined membranes became impermeable to N_2 and were filled with small, dense particles of MCM-41. All the pore was completely blocked by silica and surfactant. Figure 6 displays the transmembrane pressure vs gas permeance for a variety of gases, including CO_2, N_2, CH_4, He, and H_2. The permeability of a material decreases as the square root of its molecular weight. shown in Figure 6 with standard error of regression about 1.03 % proving that the diffusion mechanism is Knudsen flow. Pure gases consistently pass through the MCM-41 membrane with a pressure drop, demonstrating that viscous flow does not contribute to total permeance. The membranes contain a tiny pinhole brought on by viscous flow. To be attractive as a membrane for a wide range of applications, it must have

high permeability and high selectivity. The Knudsen diffusion is a phenomenon that appears when the average distance between intermolecular collisions in the gas phase is significantly greater than the average distance between pore walls. As a result, transport happens when diffusing molecules collide with the pore walls. The composition of porous support is frequently connected to Knudsen's diffusion coefficient. The permselectivity of the membrane in the Knudsen method is consequently equal to the square root of the reciprocal of the molecular weight ratio[25,26].

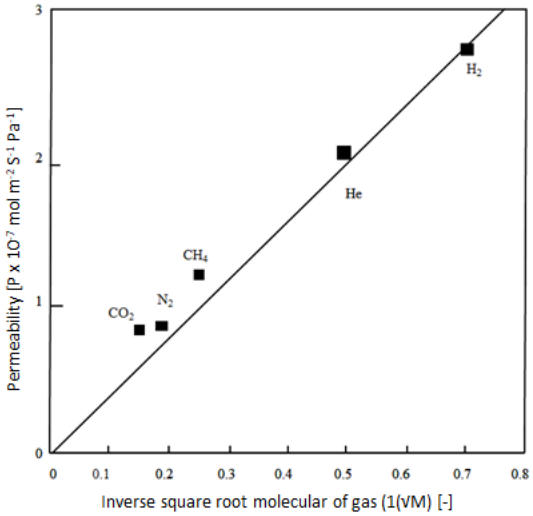

Fig. 6: Permeability Vs inversely square root molecular weight of some gases

The correlation graph between the diffusive flow and the relative water vapor pressure for membrane is shown in Figure 7. As the pressure of the water grew, the flux of nitrogen through the membrane decreased proportionally to the vapor pressure of the water. This shows that the membrane has a narrow pore size distribution, which is perfect for boosting nitrogen transfer efficiency. From the sharp decrease results, indicated that there is no big pinhole or cracks in the synthesized membrane[27]. The Kelvin radius, which is used to determine the actual pore radius, must be accurate for the adsorbed t-layer. This t-layer is determined from independent adsorption investigation carried out on non-porous surfaces, which are done using homogeneous methods. However, because these methods are specific to laboratories, an approximation was made when calculating the t-layer directly from the permporometry data. According to data as shown in Figure 8, Kelvin diameter was calculated about 2.5 nm. The real pore size may be around 3 nm when taking into account the presence of a t-layer for permporometric assessment.

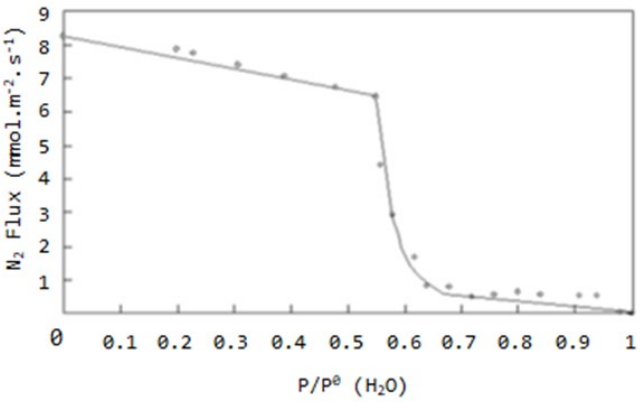

Fig. 7: Permporometry of MCM-41 membrane

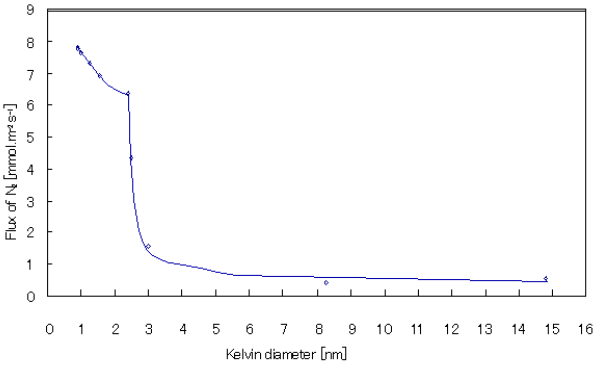

Fig. 8: Kelvin Diameter of synthesized MCM-41 membrane

4. Conclusions

The hexagonal pore structure of MCM-41 membranes was able to be created on alpha-alumina support by dip coating. The average BJH pore size in the synthesized membrane was around 2 nm, and it had a narrow pore size distribution. Since the overall permeance of pure gases through MCM-41 membranes was constant with pressure drop, there was no supply of viscous flow. Gas permeability was inversely correlated with molecular weight square root. Diffusion mechanism is Knudsen flow. The structures have a good stability in high temperature and low pH condition. Pore pressure below 900 psi causes the permeability to rise as the pressure drops more. Since their effects are more pronounced at low pore pressures, Knudsen diffusion and slip flow dominate the permeability shift in this regime. This result was open the wide application for upgrading biogas.

Acknowledgements

The authors would like to thank to the Indonesian government for the financial support and facilities to complete this work in accordance with Decree no 27/HK/2022.

References

1) C.S. Wibowo, A. Fransiskus, Y.S. Nugroho, B.

Sugiarto, " The Optimization of The Relationship between Octane Number of Gasoline-Ethanol Blen"d Fuels in Various Settings of The Engine Control Module", Evergreen Joint Journal of Novel Carbon Resource Sciences & Green Asia Strategy, Vol.07, Issue 04, pp587-592 (2020). https://doi.org/10.5109/4150510

2) K. Baz, D. Xu, H. Ali, U. Khan, J. Cheng, K. Abbas, I. Ali, " Nexus of minerals-technology complexity and fossil fuels with carbon dioxide emission: Emerging Asian economies based on product complexity index", J. Cleaner Production 373(2022)133703
3) C. Mulder, E. Conti, G. Mancinelli, " Carbon budget and national gross domestic product in the framework of the Paris Climate Agreement", Ecological Indicators 130(2021)108066
4) D.F. Hakam, H. Nugraha, A. Wicaksono, R.A. Rahadi, S.P. Kanugrahan, " Techno-Economic Analysis of Indonesia Power Generation Expansion to Achieve Economic Sustainability and Net Zero Carbon 2050" Energy Strategy Reviews 41(2022)100856
5) O.W. Awe, Y. Zhao, A. Nzihou, D.P. Minh, N. Lyczko, " A Review of Biogas Utilisation, Purification and Upgrading Technologies", Waste and Biomass Valorization, Springer, 2017, 8 (2), p.267-283. 10.1007/s12649-016-9826-4. hal-01619254
6) I.B., Dalha, M.A. Said, Z.A.A. Karim and S.E. Mohammed, "Effects of High CO2 Contents on the Biogas/Diesel RCCI Combustion at Full Engine Load", EVERGREEN Joint Journal of Novel Carbon Resource Sciences & Green Asia Strategy, Vol. 09, Issue 01, pp49-55 (2022) https://doi.org/10.5109/4774216
7) E.R. Finalis, J. Prasetyo, N. Rahmawati, T.P. Rini, Z.D. Hastuti, N. Valentino, S. Patisenda, "Development of Bio-CSTR Design For Bio-H2 From POME As Renewable Fuel", EVERGREEN Joint Journal of Novel Carbon Resource Sciences & Green Asia Strategy, Vol. 09, Issue 02, pp491-499 (2022). https://doi.org/10.5109/4794177
8) M. Lafratta, R.B.Thorpe, S.K.Ouki, A. Shana, E. Germain, M. Willcocks, J. Lee, " Development and validation of a dynamic first order kinetics model of a periodically operated well-mixed vessel for anaerobic digestion", Bioresource Technology, 2020, 310, 123415
9) M. Ayadi, S. Ahou, S. Awad, M. Abderrabba, Y. Andres, "Production of Biogas from Olive Pomace", EVERGREEN Joint Journal of Novel Carbon Resource Sciences & Green Asia Strategy, Vol. 07, Issue 02, pp228-233 (2020). https://doi.org/10.5109/4055224
10) B.C. Gandara, O.G. Depraect, F.S. Beneit, S. Bordel, R. Lebrero, R. Munoz, " Recent trends and advances in biogas upgrading and methanotrophs-based valorization", Chemical Engineering Journal Advances, 2022, 11, 100325
11) J. Zhao, Y. Li, R. Dong, " Recent progress towards in-situ biogas upgrading technologies", Science of the Total Environment, 2021, 800, 149667
12) J. Zhang, Y. Li, B. Wu, X. Huang, Z. Hou, R. Chen, " Performance and mechanism of in-situ biogas upgrading using anaerobic membrane bioreactor effluent", Journal of Water Process Engineering 44 (2021) 102323
13) M. Bozorg, Á.A.R. Santos, B. Addis,V. Piccialli, C. Castel, E. Favre, " Optimal process design of biogas upgrading membrane systems: Polymeric vs high performance inorganic membrane materials", Chemical Engineering Science, 2020, 225, 115769
14) K.N. Szmajda, A.W. Grabczyk, A. Jankowski, U. Szeluga, M. Wójtowicz, J. Konieczkowska, A. Hercog, " Gas transport properties of mixed matrix membranes based on thermally rearranged poly(hydroxyimide)s filled with inorganic porous particles", Separation and Purification Technology, 2020, 242, 116778
15) Y. Wibisono, A. Amanah, A. Sukoyo, F. Anugroho, E. Kurniati, "Activated Carbon Loaded Mixed Matrix Membranes Extracted from Oil Palm Empty Fruit Bunches for Vehicle Exhaust Gas Adsorbers", EVERGREEN Joint Journal of Novel Carbon Resource Sciences & Green Asia Strategy, Vol. 08, Issue 03, pp593-600 (2021). https://doi.org/10.5109/4491651
16) S. Yua, S. Li, Y. Liu, S. Cui, X. Shen, " High-performance microporous polymer membranes prepared by interfacial polymerization for gas separation", Journal of Membrane Science, 2019, 573, 425-438
17) M.U. Khan, J.T.E. Lee, M.A. Bashir, P.D. Dissanayake, Y.S. Ok, Y.W. Tong, M.A. Shariati, S. Wu, B.K. Ahring, " Current status of biogas upgrading for direct biomethane use: A review", Renewable and Sustainable Energy Reviews, 2021, 149, 111343
18) S.N. Mithra, S.S. Ahankari, " Nanocellulose-based membranes for CO2 separation from biogas through the facilitated transport mechanism: a review", Materials Today Sustainability 19 (2022) 100191
19) S. Ali, B. Hua, J.J. Huang, R.L. Droste, Q. Zhou,W. Zhao, L. Chen, " Effect of different initial low pH conditions on biogas production, composition, and shift in the aceticlastic methanogenic population", Bioresource Technology 289 (2019) 121579
20) B. Karimi, N. Ganji, O. Pourshiani, W.R. Thiel, "Periodic mesoporous organosilicas (PMOs): From synthesis strategies to applications", Progress in Materials Science, 2022, 125, 100896
21) S. Dou, L. Hao, H. Liu, " A mesoscopic model for simulating the physisorption process in nanopores", Chemical Engineering Science 262 (2022) 117988
22) X. Chen, M.F. Hossain, C. Duan, J. Lu, Y.F. Tsang,

M.S. Islam, Y. Zhou, " Isotherm models for adsorption of heavy metals from water - A review", Chemosphere 307 (2022) 135545

23) S.G. Aspromonte, A.V. Boix, " Improving of cold-start and combustion emissions in lean NO conditions with active and selective AgAl mesoporous catalysts", Journal of Environmental Chemical Engineering 7 (2019) 102995
24) S.S. Udai, P. Singh, " MCM-41-supported palladium (II) α-diimine complex: A recyclable catalyst for Suzuki-Miyaura coupling reaction", Results in Chemistry 3 (2021) 100189
25) J. Joseph, G. Kuntikan, D.N. Singh, " Investigations on gas permeability in porous media", Journal of Natural Gas Science and Engineering 64 (2019) 81–92
26) H.H. Liu, J. Zhang, " An efficient laboratory method to measure the combined effects of Knudsen diffusion and mechanical deformation on shale permeability", Journal of Contaminant Hydrology 232 (2020) 103652
27) T.F. Oliveira, M.L.P. Silva, A.L. Lopes-Moriyama, C.P. Souza, " Facile preparation of ordered mesoporous Nb,Ta-MCM-41 by hydrothermal direct synthesis using columbite ore as metal source", Ceramics International 47 (2021) 29509-29514